

1. Introduction

Pancake structures found in the terrestrial equatorial stratosphere are considered to be an inertial instability phenomenon (Hitchman et al., 1987; Hayashi et al., 1998). This disturbance clearly shows a non-symmetric structure on horizontal plane (right red rectangle in Fig. 1). However, so-called "inertial instability" is a symmetric instability in rotating system.

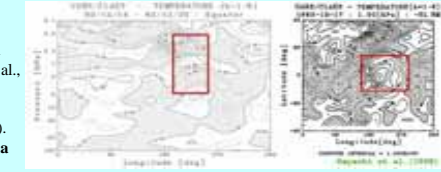


Fig. 1. Anomalies of the temperature (Left: vertical structure, Right: horizontal structure) in equatorial stratosphere from the data of satellite, UARS.

2. Recent Investigations & Our Motivations

In theoretical studies, linear stability problem for zonal symmetric flow on an equatorial beta-plane is solved by Boyd and Christidis (1982), Stevens (1983), Dunkerton (1983). These studies have shown that

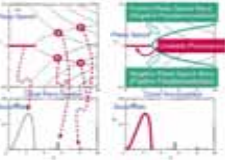
- the condition for symmetric disturbances is derived.
- non-symmetric disturbances dominate symmetric disturbances.

However, it has not been well examined whether non-symmetric instability correspond to symmetric inertial instability. Then, the purpose of our study is as follows:

- To investigate unstable mode for wide parameter range
- To examine the physical mechanism of non-symmetric and symmetric unstable modes.
- To discuss whether the non-symmetric unstable modes have the same mechanism as symmetric inertially unstable modes.

3. Approach

We firstly solve the linear stability problem. Next, dispersion relations of modes are examined from the viewpoint of resonance between neutral waves (Cairns, 1979; Hayashi and Young, 1987; Iga, 1999).



- The concepts:
- Instability is caused by resonance between the wave with positive pseudomomentum and the wave with negative pseudomomentum (Cairns, 1979).
 - The sign of the pseudomomentum M of neutral modes is determined by the gradient of dispersion curve ($k-Cr$), that is, $dCr/dk < 0$ ($dCr/dk > 0$) $M > 0$ ($M < 0$) (Iga, 1999a).
 - Continuous modes have pseudomenta with opposite sign to the gradient of the potential vorticity of basic flow by Iga (1999b).

Fig. 2. Dispersion curves on ($k-Cr$) and ($k-kCI$)-planes. From Hayashi and Young (1987).

4. Configurations & Equations

We use non-dimensional shallow water equations on an equatorial beta-plane.

$$\begin{cases} \frac{\partial u'}{\partial t} + \bar{u} \frac{\partial u'}{\partial x} + v'(1-\gamma) = -\frac{\partial \phi'}{\partial x}, \\ \frac{\partial v'}{\partial t} + \bar{u} \frac{\partial v'}{\partial x} + \bar{v} u' = -\frac{\partial \phi'}{\partial y}, \\ \frac{\partial \phi'}{\partial t} + \bar{u} \frac{\partial \phi'}{\partial x} + \frac{1}{E} \left(\frac{\partial u'}{\partial x} + \frac{\partial v'}{\partial y} \right) = 0. \end{cases} \quad \text{where } E \equiv \frac{\gamma^2 E}{\beta^2}, \quad \left(\gamma = \frac{\partial \bar{u}}{\partial y}, E \equiv \frac{m^2}{N^2} = \frac{1}{gH} \right)$$

by expanding variables in $e^{i(kx - \omega t)}$

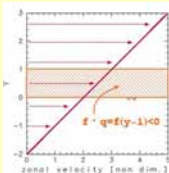


Fig. 3. A basic state and inertially unstable region.

- Boundary Condition: $v' = 0$
- Basic state: linear shear flow: $\bar{u} = y + 2$
- Zonal wavenumber range: $0 \leq k \leq 1$
- Range of E : $-2.5 \leq \log E \leq 7.5$

5. Result (Summary) — Classification of unstable modes

Inertially unstable modes are caused by resonance between equatorial Kelvin modes and westward mixed Rossby-gravity modes.

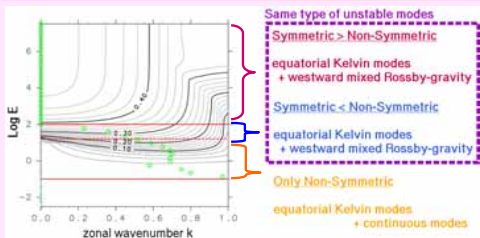


Fig. 4. Non-dimensional growth rate as a function of k and $\log E$. Green circle indicates the most unstable mode for each $\log E$.

A. Non-symmetric unstable region ($-1.0 < \log E < 1.2$)

A.1 Dispersion curves

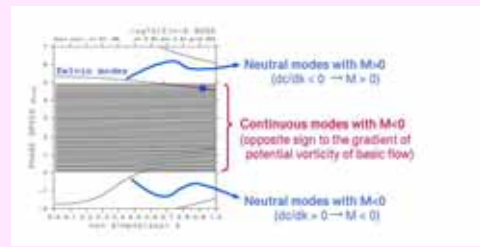


Fig. 5. Dispersion curves of neutral and unstable modes at $\log E = -0.90$. Single and double open circles indicate unstable modes and the most unstable modes, respectively.

A.2 Neutral waves leading to instability

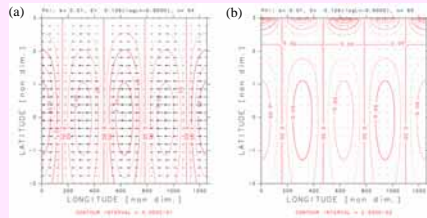


Fig. 6. Horizontal structures of modes leading to the most unstable modes for $\log E = -0.90$. (a) equatorial Kelvin mode with $k=0.01$, (b) continuous modes with $k=0.01$, (c) 4.90. Contours and vectors indicate the velocity field, respectively. Contour intervals are (a) 0.50, (b) 0.12. Dashed contours correspond to negative values.

A.3 For larger value of log E case

For larger value of E , dispersion curves of the most unstable modes are buried in continuation mode. Identification of neutral modes becomes impossible by the previous method.

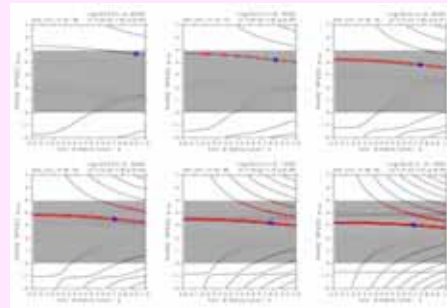


Fig. 7. Same as Fig. 5, but for $\log E = -0.90$ to 1.10.

A.4 Identification of the dispersion curves buried among continuous modes (Part 1)

In order to identify the dispersion curves of equatorial Kelvin modes, we derive approximate dispersion relation of modes. With these approximation, $v' = 0$ (for applying to equatorial Kelvin wave), modified basic flow involving in advection term: $\omega - k\bar{u}(y) \approx \omega - k \times \bar{u} \approx \hat{\omega}$, where \bar{u} with tilde is set to be the velocity of basic flow at the dynamic equator, 2.5.

$$\begin{cases} -\hat{\omega} u' = -k \phi', \\ \hat{\omega} v' = -\frac{\partial \phi'}{\partial y}, \\ -\hat{\omega} \phi' = -\frac{k v'}{E} \end{cases} \quad c = \frac{\omega}{k} = \bar{u} + \frac{1}{\sqrt{E}}$$

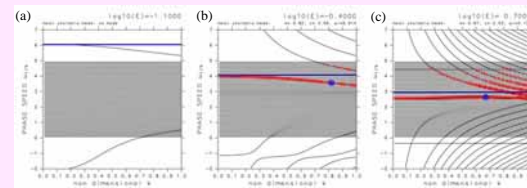


Fig. 8. Approximate dispersion curves of equatorial Kelvin wave modes (blue line) and numerically obtained dispersion curves. Values of $\log E$ are (a) -1.10, (b) -0.40, and (c) +1.10. Single and double open circles indicate unstable modes and the most unstable modes, respectively.

A.5 Identification of the dispersion curves buried among continuous modes (Part 2)

By applying Iga (1999), we solve eigenvalue problems where part of the basic flow is distorted and extract equatorial Kelvin modes directly from continuous modes into which equatorial Kelvin modes assimilate.

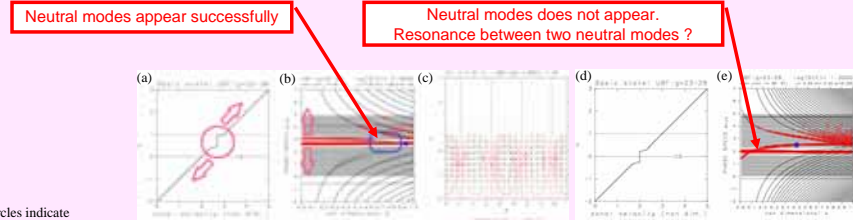


Fig. 9. Basic flows with uniform velocity regions (a), (d), and the resulting dispersion curves (b), (e). (c) shows the structure of neutral mode in blue rectangle of (b). Contours and vectors indicate the velocity field, respectively in (b).

B. Non-symmetric modes dominate case ($1.2 < \log E < 2.0$)

B.1 Dispersion curves

In the neighborhood of $\log E = 1.0$, the dispersion curves of the most unstable modes intersect that of westward mixed-Rossby gravity modes.

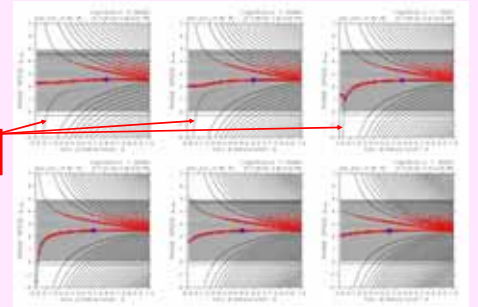


Fig. 10. Same as Fig. 5, but for $\log E = 0.90$ to 1.40.

B.2. To identify Mixed Rossby-Gravity modes

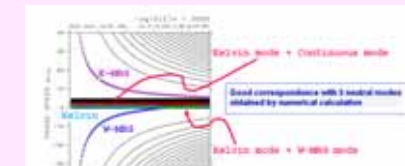


Fig. 11. Approximate dispersion curves (purple, light blue, and blue lines) and numerically obtained dispersion curves for $\log E = 1.00$.

As $\log E$ becomes large, resonance between equatorial Kelvin modes and westward mixed Rossby-gravity modes occurs at smaller zonal wavenumber region (not shown). At $\log E = 1.20$, that resonance occurs at all zonal wavenumber region except for $k=0$.

C. Connection of non-symmetric modes to inertially unstable modes

The unstable mode of $k=0$ certainly exists on the dispersion curve of the most unstable mode caused by the resonance between equatorial Kelvin modes and westward mixed Rossby-gravity modes. Although not shown here, it also confirmed that the approximate complex frequency of this non-symmetric unstable modes given by $\omega - k\bar{u}$ approximation, coincides with that of symmetric modes on the limit of k close to 0. Therefore, it is identified that non-symmetric unstable modes in the range of $1.00 < \log E < 2.00$ can be considered to be same kind of instability as the inertially unstable modes.

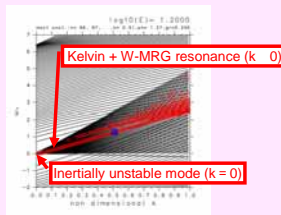


Fig. 12. Same as Fig. 5, but for $\log E = 1.00$ on (k, r)-plane.